Supporting Information

Probing the Influence of Morphological Transformation on the Electrochemical Properties of Hydrated Tungsten Oxide ($WO_{3-x}.H_2O$) for High-Rate Aqueous Asymmetric Supercapacitor

Harishchandra S. Nishad,[a] Shobhnath P. Gupta,[a] Aruna Ivaturi,[b] Pravin S. Walke [a,b*]

[a]National Centre for Nanosciences and Nanotechnology, University of Mumbai, Mumbai, 400098, India.

[b]Smart Materials Research and Device Technology Group, Department of Pure and Applied Chemistry, University of Strathclyde, Glasgow G1 1XL, UK.

Corresponding Email: shivshripsw@gmail.com

1.1 Working electrode preparation

The working electrode was prepared by adding 5 mg of sample in 2 mL solution of deionized water and ethanol (1:1 ratio), along with 10 µL of nafion as a binder. The resulting mixture was sonicated for 5 minutes, afterwards 10 µL of the solution was loaded onto a glassy carbon electrode. The electrode was further dried under an IR lamp (200 W).

1.2 Mass Balancing for AASC device fabrication

For the fabrication of an asymmetric supercapacitor, charge balancing is achieved using the below Equation S1:

$$\frac{M^{+}}{M^{-}} = \frac{C_s^{-}}{C_s^{+}} x \frac{\Delta V^{-}}{\Delta V^{+}} \qquad \text{(S1)}$$

Here, C_s^+ and C_s^- represent the specific capacitance values of the positive and negative electrodes, respectively, while ΔV^+ and ΔV^- denote their corresponding potential windows. The specific capacitance, energy density, and power density were calculated using Equations S2, S3, S4, and S5.

1.3 Specific Capacitance by GCD,

$$C_S = \frac{I\ x\ \Delta t}{m\ x\ \Delta V} \quad (\text{F g}^{-1}) \qquad \text{(S2)}$$

where, I - Current (A), m - Mass loading on electrode, Δt - time (s), ΔV - Potential Window (V),

1.4 Specific capacitance by CV,

$$C_S = \frac{1}{2.m.v.\Delta V} \int_{Vmin}^{Vmax} I(V)dv \quad (F\ g^{-1}) \qquad (S3)$$

where, C_s is the specific capacitance, m is the mass of active materials, V_{max} and V_{min} is the operational potential window, and I is current.

1.5 Energy density,

$$E_g = \frac{Cs\ X\ V^2}{2\ x\ 3600} \quad (W\ h\ kg^{-1}) \qquad (S4)$$

C_s represents the specific capacitance ($F\ g^{-1}$), while V denotes the potential window (V).

1.5 Power Density,

$$P = \frac{Eg\ x\ 3600}{\Delta t} \quad (W\ kg^{-1}) \qquad (S5)$$

E_g represents the energy density ($W\ h\ kg^{-1}$), while Δt denotes the time.

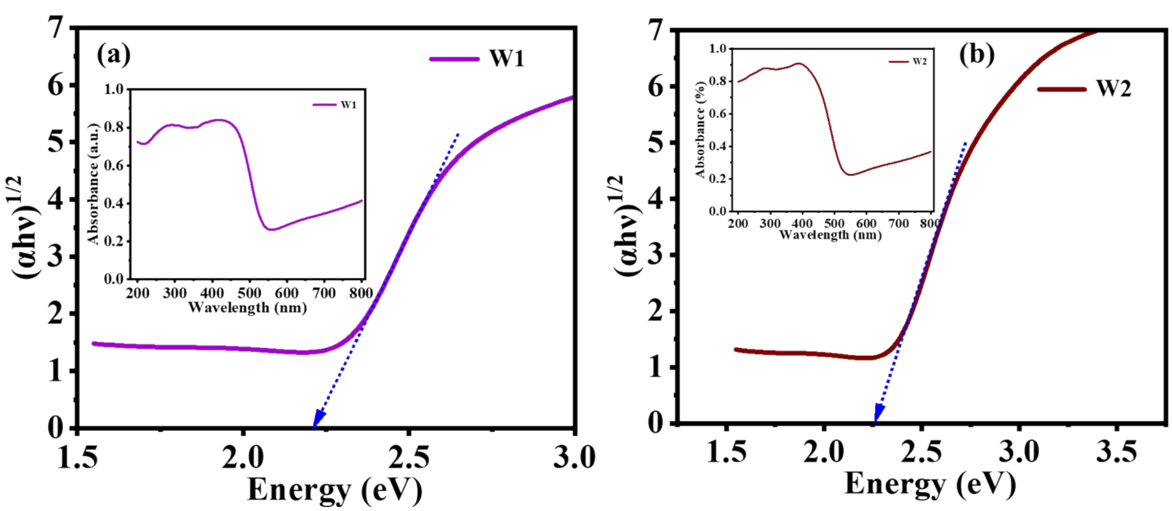

Fig. S1 (a) Tauc plot of W1 and inset represent absorbance spectra of W1, (b) Tauc plot of W2 and inset is absorbance spectra of W2.

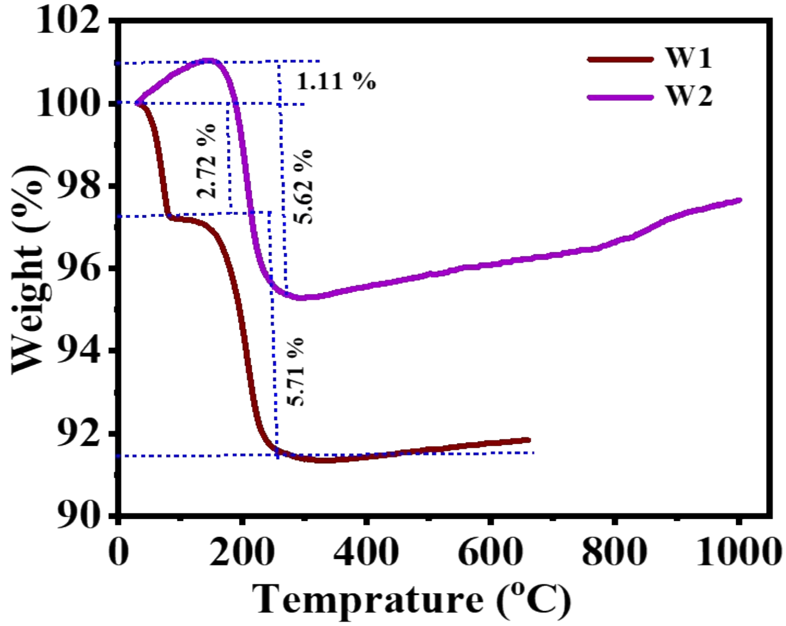

Fig. S2 TGA spectra of W1 and W2.

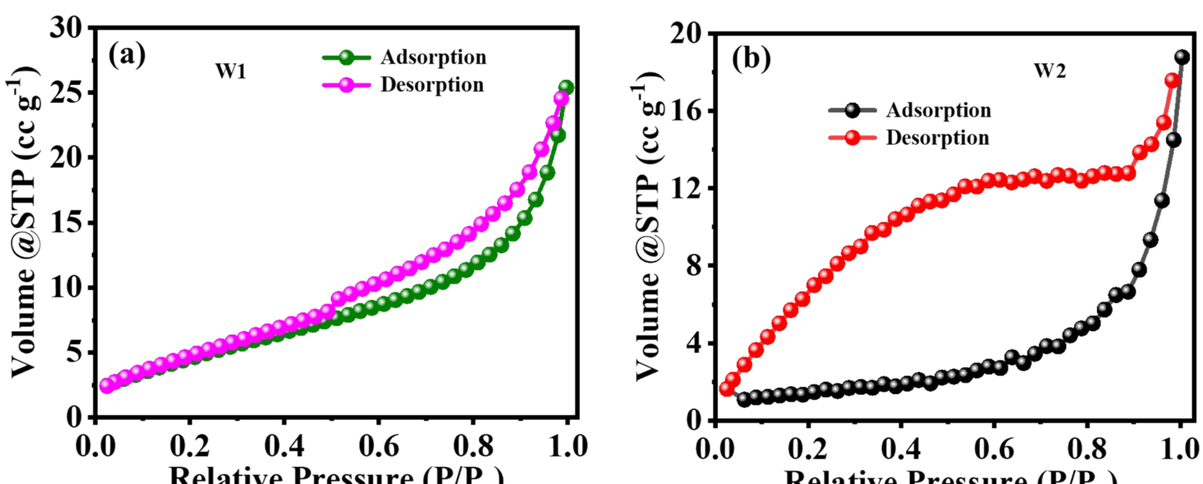

Fig. S3 Nitrogen adsorption-desorption isotherm of W1 (a) and W2 (b).

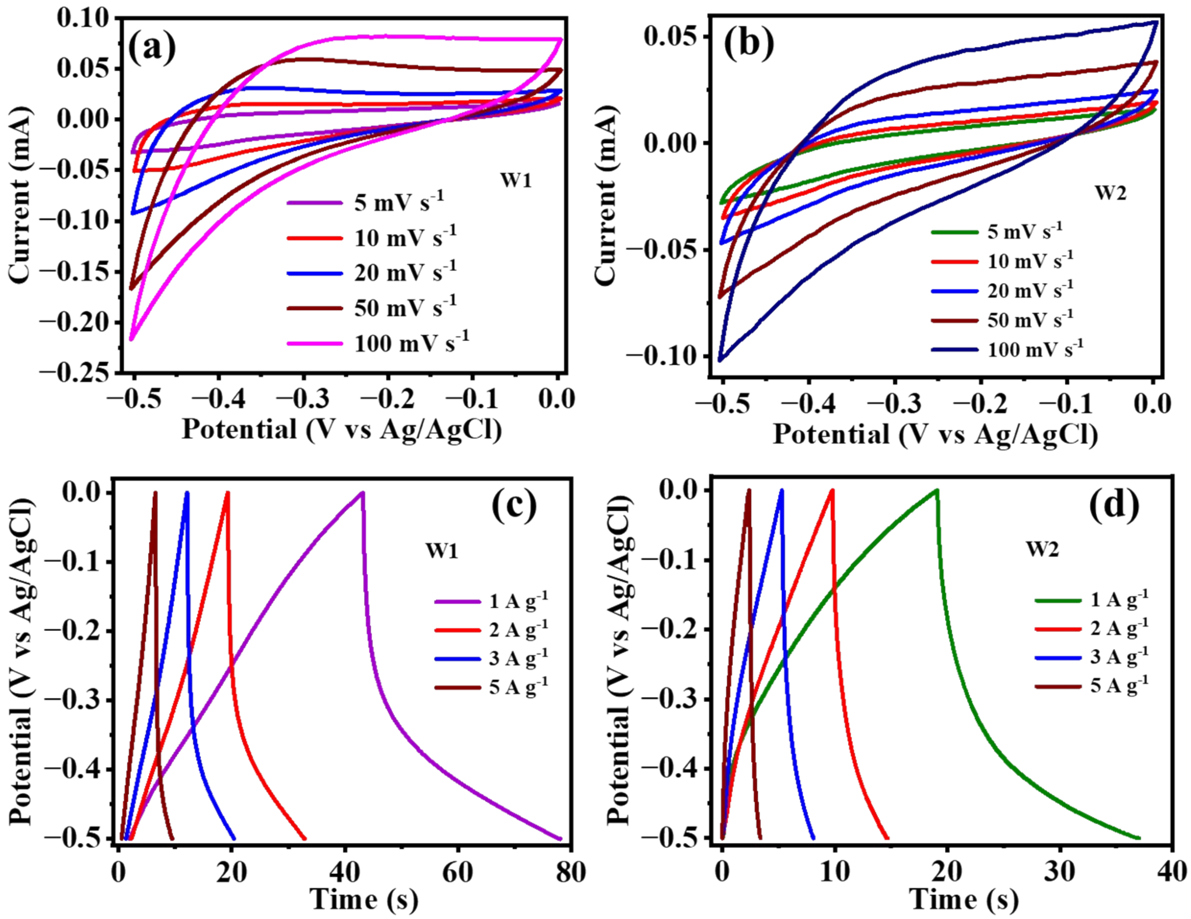

Fig. S4 (a, b) CV curves, (c, d) GCD curves of W1 and W2 respectively.

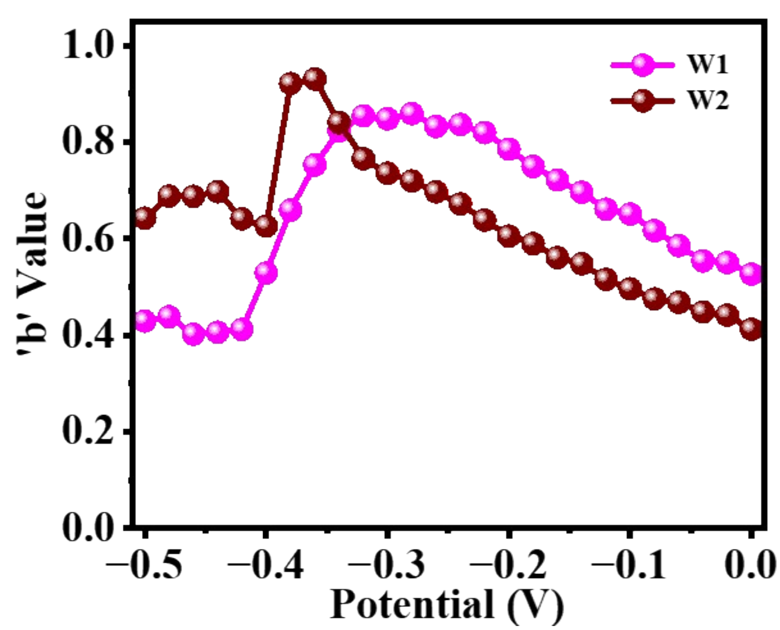

Fig. S5 'b' values at different potentials of W1 and W2 respectively.

Table (S1): Electrochemical results of W1 and W2 by three electrodes.

Sr. No.	Sample	Electrolyte	Potential	C_s (F g^{-1})	Diffusion Coefficient (D)	R_s (Ω)	R_{ct} (Ω)	Z_w (Ω)
1.	W1	1 M H_2SO_4	0 V to -0.5 V	70 @ 1 A g^{-1}	4.77 x 10^{-4} cm^2 s^{-1}	0.25	1.91	2.17
2.	W2	1 M H_2SO_4	0 V to -0.5 V	37 @ 1 A g^{-1}	2.43 x 10^{-4} cm^2 s^{-1}	0.26	2.41	2.66

Table (S2): Comparison of available literature of $WO_3.H_2O$.

Sr. No	Material	Method	Morphology	Electrolyte	C_s (F g^{-1})	Stability (%) @ cycles	Ref.
1.	$WO_3.H_2O$	Wet-Chemical	Nanoflower	0.5 M H_2SO_4	71 @ 2 A g^{-1}	-	[1]
2.	$WO_3 \cdot H_2O$	Hydrolysis	-	1 M $LiClO_4$	78.5 @ A g^{-1}	73 @300	[2]
3.	$WO_3 \cdot H_2O$	Hydrothermal	Nanorod	1 M H_2SO_4	460 @1 A g^{-1}	93 @2000	[3]
4.	$WO_3 \cdot H_2O$	Wet-Chemical	Nanoplate	1 M H_2SO_4	160 @ 2 mV s^{-1}	87 @2500	[4]
5.	$WO_3 \cdot H_2O$	Hydrothermal	Nanoflower	1 M H_2SO_4	140 @ 1 A g^{-1}	97 @900	[5]
6.	$WO_3 \cdot H_2O$	Wet-Chemical	Nanoplate	1 M H_2SO_4	606 @ 1 A g^{-1}	83 @4000	[6]
7.	$WO_3 \cdot H_2O$	Wet-Chemical	Nanoslab	1 M H_2SO_4	386 @ 1 A g^{-1}	96 @3000	[7]
8.	$WO_3 \cdot H_2O$	Wet-Chemical	Nanodisk	1 M H_2SO_4	255 @ 1 A g^{-1}	-	[8]
9.	**$WO_3 \cdot H_2O$ (W1)**	**Wet-Chemical**	**Nanoflowers**	**1 M H_2SO_4**	**70 @ 1 A g^{-1}**	**97 @5000**	**This work**
10.	**$WO_3 \cdot H_2O$ (W2)**	**Wet-Chemical**	**Nanoribbon**	**1 M H_2SO_4**	**37 @ 1 A g^{-1}**	**-**	

References

[1] Le P A, Le V Q, Tran T L, Nguyen N T and Phung T V B 2022 Computation and Investigation of Two-Dimensional $WO_3 \cdot H_2O$ Nanoflowers for Electrochemical Studies of Energy Conversion and Storage Applications *ACS Omega* **7** 10115–26

[2] Koo B R, Jo M H, Kim K H and Ahn H J 2021 Amorphous-quantized $WO_3 \cdot H_2O$ films as novel flexible electrode for advanced electrochromic energy storage devices *Chem. Eng. J.* **424** 130383

[3] Gupta S P, More M A, Late D J and Walke P S 2021 Highly ordered nano-tunnel structure of hydrated tungsten oxide nanorods for superior flexible quasi-solid-state hybrid supercapacitor *Appl. Surf. Sci.* **545** 149044

[4] Nishad H S, Gupta S P, Kotha V, Patil B M, Chakane S D, Bute M G, Gosavi S W, Late D J and Walke P S 2022 Enhanced van-der Waals separation in hydrated tungsten oxide nanoplates enables superior pseudocapacitive charge storage *J. Alloys Compd.* **914** 165227

[5] Ma L, Zhou X, Xu L, Xu X, Zhang L, Ye C, Luo J and Chen W 2015 Hydrothermal preparation and supercapacitive performance of flower-like $WO_3 \cdot H_2O$/reduced graphene oxide composite *Colloids*

Surfaces A Physicochem. Eng. Asp. **481** 609–15

[6] Gupta S P, Nishad H H, Chakane S D, Gosavi S W, Late D J and Walke P S 2020 Phase transformation in tungsten oxide nanoplates as a function of post-annealing temperature and its electrochemical influence on energy storage *Nanoscale Adv.* **2** 4689–701

[7] Gupta S P, Nishad H H, Patil V B, Chakane S D, More M A, Late D J and Walke P S 2020 Morphology and crystal structure dependent pseudocapacitor performance of hydrated WO_3 nanostructures *Mater. Adv.* **1** 2492–500

[8] Nishad H S, Gupta S P, Khan N S, Biradar A V., Lee J, Mane S M and Walke P S 2023 Structural Transformation of Hydrated WO_3 into $SnWO_4$ via Sn Incorporation Enables a Superior Pseudocapacitor and Aqueous Zinc-Ion Battery *Energy and Fuels* **37** 7501–10